Alkali borosilicate glass for vitrification of molybdenum-rich nuclear waste

Seon-Jin Kim[a], Jung-Wook Cho[a,*]
[a]*Division of Advanced Nuclear Engineering, Department of Materials Science and Engineering, Pohang University of Science and Technology (POSTECH), Pohang, Gyeongbuk 37673, Republic of Korea*
[*]*Corresponding author: reisi-fard.1@osu.edu*

Keywords : nuclear waste glass, borosilicate glass, molybdenum, crystallization, glass structure

1. Introduction

High-level liquid radioactive waste is generated during the reprocessing of spent nuclear fuel and is composed of a mixture of various elements. To ensure long-term stability, this liquid waste requires treatment to immobilize the elements within a matrix. High-level Radioactive liquid waste can be treated into various solid forms. Among them, glass is an excellent material for use as a solidification matrix because of its small volume and excellent chemical durability. Actually, countries such as the United States, Japan, and France have selected to use glass as a solidification material for waste disposal. However, unwanted crystallization during the process can lead to equipment corrosion and a change in glass properties. Especially, molybdenum is one of the fission products generated from spent nuclear fuel, and it has particularly low solubility in borosilicate glass (1 mol%).

In borosilicate glass, molybdenum can exist in various oxidation states, but it mainly exists as a hexavalent cation. The MoO_4 group formed by bonding with four non-bridging oxygen and creating its own depolymerized region within the glass network due to the high field strength of Mo. Within this region, MoO_4 does not bind with the glass network and tends to bond with alkali or alkaline earth cations to balance its 2-charge. However, as the concentration of Mo increases, crystallization occurs, leading to separation from the glass network. When alkali molybdate crystals form in this process and contain radioactive isotopes, their high solubility has a risk of leakage of radioactive species when the glass matrix contact with groundwater.

The present study investigated the effect of alkali cation in borosilicate glass on the solubility of MoO_3 to develop glass compositions that can incorporate a large amount of Mo.

2. Methods and Results

2.1 Preparation of glass samples

In this study, the basic composition was chosen in the SiO_2–B_2O_3–Al_2O_3–Na_2O–CaO–MoO_3 system. This composition was derived by simplifying SON 68, a glass developed for immobilizing high-level radioactive waste in France. In the simplified composition, Na_2O represents the total fraction of alkali oxides (Na_2O + Li_2O + Cs_2O), and CaO represents the total fraction of alkaline-earth oxides (CaO + BaO + SrO). For each sample, 5 mol% of various alkali cation (Li, Na, K, Cs) were added, and 2 mol% of MoO_3 was immobilized. The nominal composition of the glasses (shown in Table 1) is expressed as 0.9(56 SiO_2–16 B_2O_3–4 Al_2O_3–18 Na_2O–6 CaO) – 5 MoO_3 – 5 R_2O (R=Li, Na, K, Cs) in mol%.

The chemical mixtures, weighing 8 g each, were placed in 95/5 Pt/Au crucibles and melted in an electric furnace under ambient atmospheric conditions at 1200 °C for 2 h. The obtained glass frits were melted at 1200 °C for 2 h and half of the melt was cast onto an oxygen-free copper plate to obtain glass samples (quenched glass sample), while the remaining glass frit was slowly cooled to room temperature at a rate of 1 °C/min, simulating the natural cooling process observed in industrial nuclear glass canisters (slowly cooled sample).

Table I: Nominal composition of glasses (mol %).

	L	N	K	C
SiO_2	52.08	52.08	52.08	52.08
B_2O_3	14.88	14.88	14.88	14.88
Al_2O_3	3.72	3.72	3.72	3.72
CaO	5.58	5.58	5.58	5.58
Na_2O	16.74	21.74	16.74	16.74
Li_2O	5.00	0.00	0.00	0.00
K_2O	0.00	0.00	5.00	0.00
Cs_2O	0.00	0.00	0.00	5.00
MoO_3	2.00	2.00	2.00	2.00

2.2 X-ray Diffraction (XRD)

The XRD analysis of all the samples in this study was performed using an AXS D8 Advance X-ray diffractometer from Bruker, Germany.

The results of X-ray diffraction (XRD) analysis for the quenched glass samples and slowly cooled samples are presented in Fig. 1. The quenched samples coming from the batch of Li and Cs are almost no distinct crystalline peaks, indicating that they are entirely amorphous and do not contain any Mo crystals (Fig. 1a).

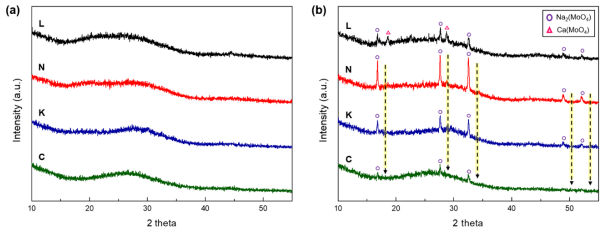

Fig. 1. XRD patterns of (a) quenched glass samples, and (b) slowly cooled samples.

On the other hand, the Fig. 1b shows the XRD results of the slowly cooled samples, revealing Na_2MoO_4 peaks in all samples. It is especially notable that when compared to the N sample, the intensity of the Na_2MoO_4 peak decreases as the alkali cation changed to K and Cs samples. Especially, in the case of the Cs sample, it can be clearly noticed a reduction in crystal peak intensity when compared to the N sample. Another finding is the presence of $CaMoO_4$ crystals only in the L sample. These XRD results show that the influence of Mo crystallization is different based on the added alkali ions.

2.3 Scanning Electron Microscopy (SEM)

The morphology of crystalline phases was analyzed using scanning electron microscopy (SEM) with a JSM-7100F instrument from JEOL.

The surface of the slowly cooled samples was analyzed using scanning electron microscopy (SEM), as shown in Fig. 2 and Fig. 3. They confirm the results obtained by XRD as it is possible to observe numerous white globules uniformly distributed in the glass. Fig. 2 presents that the white circular phase observed on the sample surface corresponds to a Na_2MoO_4 crystal-rich in Na and Mo, as revealed by the energy-dispersive x-ray spectroscopy (EDS) mapping image. This indicates that the N sample has a significant presence of the Na_2MoO_4 phase.

Fig. 3 displays the surface SEM images of the samples with different alkali cations added (Li, Na, K, Cs). In all samples, the entire surface is covered with crystals. Consistent with the XRD results (Fig. 1b), the crystalline phase predominantly formed is identified as Na_2MoO_4, rich in Na and Mo, through EDS analysis. With the previous XRD results, these SEM images indicate that the crystallization of molybdate varies depending on the added alkali.

2.4 Solid-State MAS Nuclear Magnetic Resonance Spectroscopy (NMR)

To analyze the glass structure, solid-state MAS NMR analysis was conducted on both ^{11}B and ^{27}Al for all the quenched glass samples. The analysis was performed using an Avance III HD NMR spectrometer manufactured by Bruker in Germany.

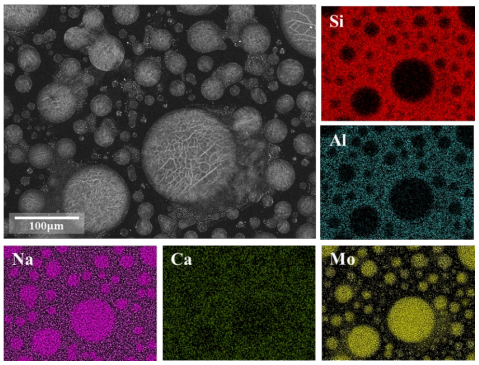

Fig. 2. SEM images with EDS elemental maps (Si, Al, Na, Ca, and Mo) obtained from the surface of the slowly cooled N sample.

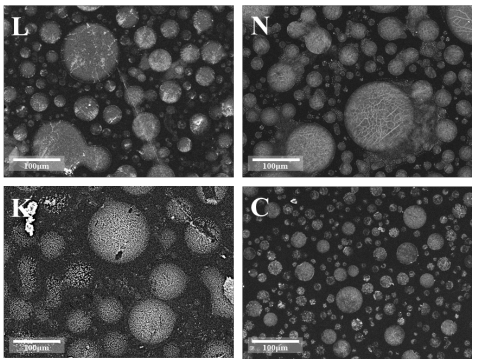

Fig. 3. SEM images of bulk samples after slow cooling from the melt at 1 °C/min.

From the solid-state MAS NMR results, the glass network structure could be further investigated with the interaction of each of the network former and network modifiers. Fig. 4 and Fig. 5 display the solid-state MAS NMR analysis for B and Al. The ^{11}B MAS spectra show the distinct two borate units of BO_3 and BO_4 (Fig. 4). The population of each B unit was calculated from simulation using the DMFit program and most of the boron exist as BO_4. In Figure 4, an increasing trend of BO_3 units was observed as the size of the added alkali ions increased. As the size of the added cations increases, it becomes more difficult for the BO_4 to charge compensate with alkali cations in the glass. So, due to the larger size of the added ions, the existing BO_4 structures can no longer compensate for charges and thus transform into BO_3.

In Fig. 5, all of the ^{27}Al MAS NMR spectra show an almost AlO_4 unit near 55 ppm but have asymmetric and broad line shapes with a long tail to low frequency. The simultaneous feature observed in both ^{11}B NMR and ^{27}Al is the occurrence of a shift towards the lower end of the chemical shift scale in the samples with added Cs. In NMR analysis, shifting peaks to lower ppm indicates stronger electron density around the element. In the case of boron, it is suggested that this effect can be linked to

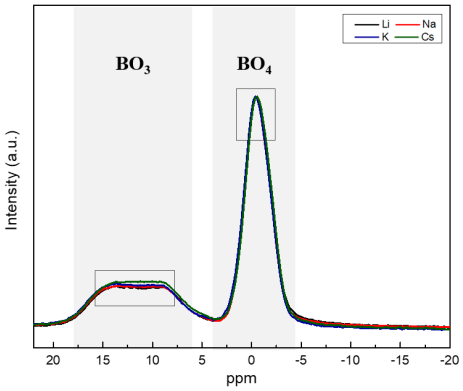

Fig. 4. ^{11}B MAS NMR spectra.

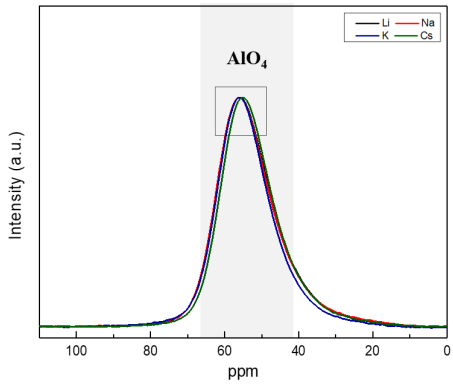

Fig. 5. ^{11}B MAS NMR spectra.

the relative decrease of B surrounded by three Si and one B, compared to B surrounded by four Si. In short, the peak shift suggests that there are more connections between B and Si in the C sample compared to other samples. Similarly, in the case of Al, although the peak width remains constant, the overall peak shift indicates that the glass environment around Al has changed. This suggests that the bonding and interactions involving Al and its neighboring elements within the glass have been changed, leading to peak shifts.

In alkali-rich alumino-borosilicate glass, when the larger alkali cation is added, it is more difficult for the elements to diffuse, resulting in an overall homogenous structure. This homogeneous glass structure can inhibit phase separation and delay crystallization. From these NMR results, it is evident that adding larger ions leads to a more abundant connection between Si, B, and Al, and makes a more uniform glass structure.

2.5 Raman spectroscopy

Raman data was collected from the quenched glass samples. Raman spectroscopy was performed at room temperature using a Raman Spectrometer (LabRaman Aramis, Horiba Jobin-Yvon, France). The spectral range analyzed was 200–1600 cm^{-1}.

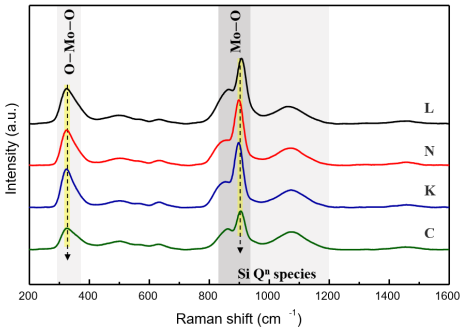

Fig. 6. Collected Raman spectra of quenched glasses.

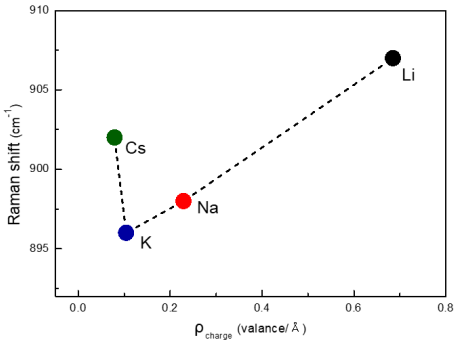

Fig. 7. Mo-O stretch band's raman shift versus network modifying cation charge density for the glass samples.

With the previous NMR results, Raman analysis can show the local environment around molybdenum. In Fig. 6, two peaks are observed for the MoO_4 unit: the first one at around 320 cm^{-1} corresponding to internal vibrational modes, and the second one at around 900 cm^{-1} representing stretching vibrational modes. These two peaks show intensity differences according to the amount of MoO_4 units. Based on the graph, we can understand that as the size of the alkali ions increases, the formation of MoO_4 decreases.

In particular, the peak around 900 cm^{-1} is highly influenced by the surrounding network related to MoO_4. It's known that the frequency shifts to higher regions when the field strength of the cation increases which is in charge compensation. Considering this fact, in Fig. 7, when the cation changes from Li to K, the peak position decreases linearly. This suggests a strong correlation between the field strength of the cation and the peak position. However, in the case of Cs, it deviates from this linear trend. It suggests that there are strong cations around MoO_4 unexpectedly.

2.6 X-ray absorption spectroscopy (XAS)

The Mo K-edge X-ray absorption spectra were collected in the transmission mode at room temperature. The measurements were performed on beamline 10C of the Pohang Light Source in South Korea. A double crystal Si (1 1 1) monochromator was used for the

experiment. The Pohang Light Source ring was operating at 2.5 GeV with a 250 mA current.

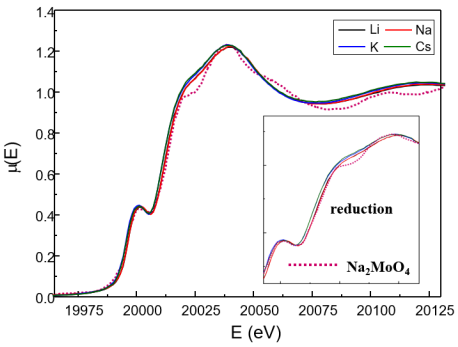

Fig. 8. Normalized Mo K-edge XANES spectra for the glasses.

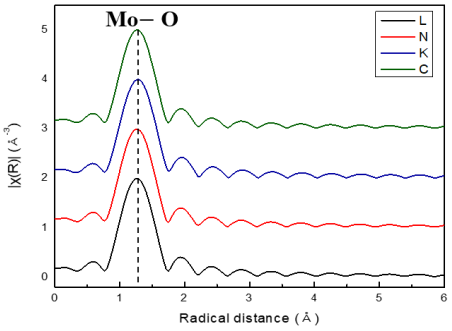

Fig. 9. Fourier transform of the EXAFS spectra of the glasses.

Table II: First-shell Mo–O fitting results for glasses. All fits used $S_0^2 = 0.92$ and $E_0 = 1.3$ eV.

	L	N	K	C
R (Å)	1.76(474)	1.76(505)	1.77(527)	1.76(710)
CN (atoms)	4.03	4.00	3.99	3.85
σ^2 (Å^2)	0.00178	0.00201	0.00154	0.00177

The results of the XAS analysis were presented to obtain information about the local environment of molybdenum. In the XAS analysis, as the size of the added alkali increased, a shift towards lower energy regions in the XANES spectrum was observed (Fig. 8). This shift can be interpreted as a reduction in the oxidation state of molybdenum. Molybdenum is mostly present as 6+ in the glass structure, but it is known that under certain compositions and conditions, a portion of it can be substituted as a 5+. There are two cases in Mo^{5+} could exist : first, they can form MoO_6 complexes and be situated within the depolymerized regions of the glass network. However, the Raman analysis did not show any peaks related to MoO_6, and the XAFS analysis also revealed a decrease in the coordination number of Mo (Fig. 9 and Table II). Therefore, this hypothesis cannot be substantiated. Second, they can act as charge compensators for MoO_4 units and enhance connectivity with the glass structure. Some studies have indicated the presence of Mo^{5+} acting as a charge compensator for MoO_4 units while assisting in connection with the silicate network. However, specific explanations regarding this have not been provided yet. We think when larger cations were added, the overall glass structure became more homogeneous, and it leads to an increase in the proportion of Mo^{5+}. And, because of the small size and high field strength, Mo^{5+} acts as a charge compensator of MoO_4. Based on the XAS data and Raman analysis, we think that, as the size of the added cations increases, the proportion of Mo^{5+} increases, and Mo^{5+} acts as a charge compensator for MoO_4 and makes the connection with the silicate network. This reaction contributes to delaying the crystallization of molybdate within the glass structure.

2.7 X-ray Photoelectron Spectroscopy (XPS)

The structural coordination of molybdenum (Mo 3d) in glasses was investigated using Mo 3d X-ray photoelectron spectroscopy (XPS) experiments. The experiments were conducted using the Nexsa G2 instrument from Thermo Fisher Scientific.

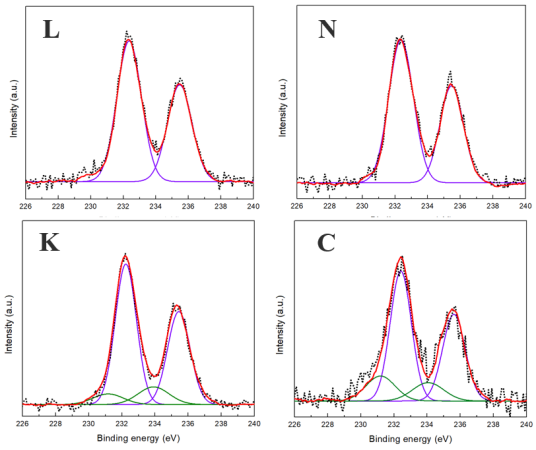

Fig. 10. XPS spectra of Mo 3d binding region.

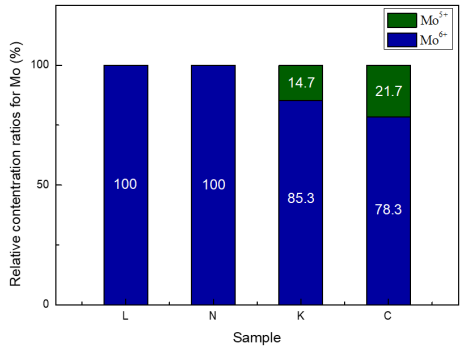

Fig. 11. XPS curve fitting results of Mo 3d.

The results of the XPS analysis also provide support for the hypothesis (Fig. 10 and Fig. 11). The results

revealed that the proportion of Mo^{5+} increased with the size of the alkali cations, with C samples showing the highest proportion of Mo^{5+}. The substitution of Mo from 6+ to 5+ occurred as larger alkali cations were added. This substitution allowed Mo to compensate for the charge of MoO_4 units while forming connections with the Si glass network, creating a more stable environment for Mo. The reason for the change in Mo oxidation state could be explained that as the cation size increases, the glass network becomes more polymerized, preventing some Mo from forming larger units like MoO_4 and leading to substitution with 5+.

3. Conclusions

As alkaline cations change from Li to Cs, the diffusion between the network former decreases, and the glass network becomes a more homogeneous glass structure because of the connection between B and Al with the Si network. Mo forms MoO_4 by bonding with four neighboring non-bridging oxygens. As the glass structure becomes more polymerized, Mo^{6+} is substituted by pentavalent Moly, and Mo^{5+} in the depolymerized region enhances connectivity with Si, acting as a charge compensator for MoO_4 rather than forming MoO_6. As a result, in Raman, a non-linear increase in field strength around MoO_4 is observed in Cs samples where Mo^{5+} is most formed. In conclusion, larger alkali cations make a more homogeneous glass structure and create an environment where Mo can be more integrated into the network. This structure delays the phase separation of Mo and allows the glass to incorporate higher Mo concentrations.

REFERENCES

[1] Caurant, D.; Majérus, O. Glasses and Glass-Ceramics for Nuclear Waste Immobilization. In Encyclopedia of Materials: Technical Ceramics and Glasses; Elsevier, 2021; pp 762–789.
[2] Nicoleau, E.; Schuller, S.; Angeli, F.; Charpentier, T.; Jollivet, P.; Le Gac, A.; Fournier, M.; Mesbah, A.; Vasconcelos, F. Phase Separation and Crystallization Effects on the Structure and Durability of Molybdenum Borosilicate Glass. Journal of Non-Crystalline Solids 2015, 427, 120–133.
[3] Caurant, D.; Majérus, O.; Fadel, E.; Lenoir, M.; Gervais, C.; Pinet, O. Effect of Molybdenum on the Structure and on the Crystallization of SiO 2 ?Na 2 O?CaO?B 2 O 3 Glasses. J American Ceramic Society 2007, 90 (3), 774–783.
[4] Ollier, N.; Charpentier, T.; Boizot, B.; Wallez, G.; Ghaleb, D. A Raman and MAS NMR Study of Mixed Alkali Na–K and Na–Li Aluminoborosilicate Glasses. Journal of Non-Crystalline Solids 2004, 341 (1–3), 26–34.
[5] (1) Mabrouk, A.; Vaills, Y.; Pellerin, N.; Bachar, A. Structural Study of Lanthanum Sodium Aluminoborosilicate Glasses by NMR Spectroscopy. Materials Chemistry and Physics 2020, 254, 123492.
[6] Calas, G.; Le Grand, M.; Galoisy, L.; Ghaleb, D. Structural Role of Molybdenum in Nuclear Glasses: An EXAFS Study. Journal of Nuclear Materials 2003, 322 (1), 15–20.
[7] (1) Chen, Z.; Meng, Z.; Liu, L.; Wang, H.; Sun, Y.; Wang, X. Structural and Viscous Insight into Impact of MoO3 on Molten Slags. Metall Mater Trans B 2021, 52 (6), 3730–3743.